Research Article

# Corrosion behavior of surface induced by wire EDM on 316L stainless steel: an experimental investigation

Raju Prathipati[1] · Ratnam Ch[2] · Siva Prasad Dora[1]




## Abstract

Wire electric discharge machining is an efficient technique among the available nonconventional machining process and is mostly used for machining complex shapes and hard materials. This process also acts as a form of surface modification technique. The discharge energy of machining process influences the nature of the machined surface to a very high degree due to high heat generation and deposition of wire electrode material. 316L stainless steel is widely used in engineering, marine and medical applications. Although 316L SS is a corrosion resistant material, there is a lot of research going on to improve its corrosion resistance by different surface modification techniques due to its applications. Investigation on the effect of WEDM parameters on the corrosion behavior of 316L SS material is carried out. Corrosion studies were carried out by Potentiodynamic polarization test and phase analysis was carried out by using XRD. Significant enhancement in the corrosion resistance of WEDMed surface is observed with the variation in pulse on time and peak current. Pulse on time and peak current are the significant parameters influencing the amount of discharge energy. Low level of discharge energy enhanced the corrosion resistance of WEDMed surface.


**Keywords** WEDM · Surface roughness · Corrosion · Discharge energy · Surface alteration

## 1 Introduction

Wire EDM plays an extensive role in current precision manufacturing environment and is used to cut conductive materials of high hardness [1]. Wire EDM is popular because of its ease and flexibility in machining complex geometrical shapes. Due to high temperatures involved in wire EDM process [2], changes on the machined surface with recast layer can be observed which in turn alters material properties [3]. Wire EDM parameters, work piece material and the material of wire electrode influences the properties of machined surface nature to a varying degree [4]. Even when different materials are machined under the same machining conditions may have different machining characteristics [5], so selection of wire EDM parameters with proper combination of values is an important and difficult task [6].

Ahmet et al. [7] presented an experimental investigation of the machining characteristics of AISI D5 tool steel in wire EDM process and found that the process energy greatly affects the surface roughness of wire EDMed material. Han et al. [8], in their investigation found that, when the pulse energy per discharge is constant, short pulses and long pulses will produce the same surface roughness but dissimilar surface morphology and different material removal rates. Surface roughness is directly proportional to the available discharge energy [9–12]. When the discharge energy was increased, the formation of thick white layer with voids and cracks were observed by Chen et al. [13] which resulted in the increase of surface roughness. An experimental investigation carried out by Newton et al. [14] on the recast layer formation on machining Inconel 718 material due to wire EDM process found that the recast layer thickness increased with energy per spark, peak discharge

✉ Raju Prathipati, prathipatiraju25@gmail.com | [1]Department of Mechanical Engineering, GITAM Deemed to be University, Visakhapatnam, India. [2]Department of Mechanical Engineering, Andhra University, Visakhapatnam, India.

SN Applied Sciences (2019) 1:952 | https://doi.org/10.1007/s42452-019-0992-4

Received: 14 June 2019 / Accepted: 26 July 2019 / Published online: 1 August 2019

current, and current pulse duration. The recast material was found to possess in-plane tensile residual stresses, as well as lower hardness and elastic modulus than the bulk material. The surface morphology of conventionally ground, polished and EDM-finished surfaces of dental cast alloys used for the fabrication of implants were studied by Zinelis et al. [15] and observed that the EDMed surfaces having significant increase in carbon content due to the decomposition of the dielectric fluid during spark erosion forming carbides. Deposition of copper was also noticed on these surfaces from the decomposition of the copper electrodes used for EDM. Cross-sectional analysis showed the formation of superficial recast layer. Prasad et al. [16] studied the effect of wire EDM parameters on damping behavior of machined surface and found that the parameters pulse on time and pulse off time controls damping capacity and independent of peak current. Yan et al. [17] studied the combined effect of EDM with ball burnish machining of Al–Zn–Mg alloy and found that there is improvement in surface roughness and corrosion resistance. According to Yu et al. [18] wire EDM with auxiliary pulse voltage supply is an efficient method of machining poly silicon material to achieve good quality and high efficiency. Ghanem et al. [19] studied the influence of the EDM parameters on surface integrity and found that the machined surface properties depend mainly on material type. The wire EDM parameters, work-piece and wire material strongly influence the machined surface characteristics. Machining conditions are very crucial on surface oxide layer formation and hence selection of parameters is very crucial [20]. According to Gungor et al. [21] the EDM surfaces were greatly influenced by electrode and dielectric fluid showing changes in material properties with varying process parameters. The wear resistance of EDMed austenitic steel was found to be improved because of carbides formation in the recast layer during machining. Basil et al. [22] in his investigation observed that the hardness of wire EDMed titanium alloy specimens are high due to changes in the recast layer.

The deterioration of material in the presence of environment by electrochemical or chemical factors is defined as corrosion. Material can be subjected to corrosion in a few hours or may take years [23, 24]. Generally 316L stainless steel and titanium alloys are used as implant materials because of their properties but still there is a need to improve them. The surgically removed implants show damage to the surrounding tissue due to wear and corrosion. Improving the corrosion resistance of a material will enhance the reliability of material in corrosive environments. The corrosion resistance of a material can be studied from polarization curves generated by varying the applied voltage with current density in corrosive medium. The corrosion resistance of materials mainly depends upon two key factors, the elemental composition and the porosity of the surface. Shoja et al. [25] studied the effect of corrosion resistance of titanium immersed in Hanks solution with different surface characteristics and observed that corrosion resistance decreased with increase in surface roughness. The application of hydro oxyapatite coatings improved the corrosion resistance of titanium alloy and 316L stainless steel materials [26]. Tiwari et al. [27] studied the effect of alumina coated 316L stainless steel material in ringer's solution and found the corrosion resistance to be on higher side. Uniform surface characteristics are obtained with the coated wires. According to Feng et al. [28] corrosion resistance of 316L stainless steel material improved with increase in Titanium ion implantation. According to Prasad et al. [29] nickel electroplated aluminum metal matrix composites exhibit high corrosion resistance when compared to uncoated material when tested in sodium chloride solution. Yue et al. [30] presented a paper on corrosion behavior of the machined surface of magnesium composite under different machining processes and found that the polished and fine-ground specimens show high corrosion resistance when compared to other machining process. Every machining process will induce residual stress on the surface. Wire EDM generates surface of high tensile stress effecting characteristics such as fatigue, corrosion and wear resistance [31].

Form the literature it is clearly evident that there is scope for obtaining good surface finish as well as good corrosion resistance on wire EDMed material. As limited research is available on this aspect, an attempt is made to study the effect of WEDM parameters on corrosion resistance of 316L stainless steel material.

## 2 Experimentation

### 2.1 Material

316L stainless steel is used as work piece material for the study and its chemical composition is presented in Table 1.

### 2.2 Wire electric discharge machining

For machining the specimens, Japax LDM 50 WEDM machine is used and is shown in Fig. 1a and the schematic diagram of wire EDM is shown in Fig. 1b [32]. The varying

**Table 1** Chemical composition of the material 316L SS

| S | C | P | Si | Mn | Mo | Ni | Cr | Fe |
|---|---|---|---|---|---|---|---|---|
| 0.001 | 0.017 | 0.025 | 0.56 | 1.21 | 2.16 | 11.1 | 17.6 | Bal |

parameters considered for machining are pulse on time, peak current, servo voltage and wire tension [33]. Brass wire is used as wire electrode for machining in the presence of distilled water which is considered as dielectric fluid. Specimens of size 13 × 12 × 6 $mm^3$ were machined for experimentation.

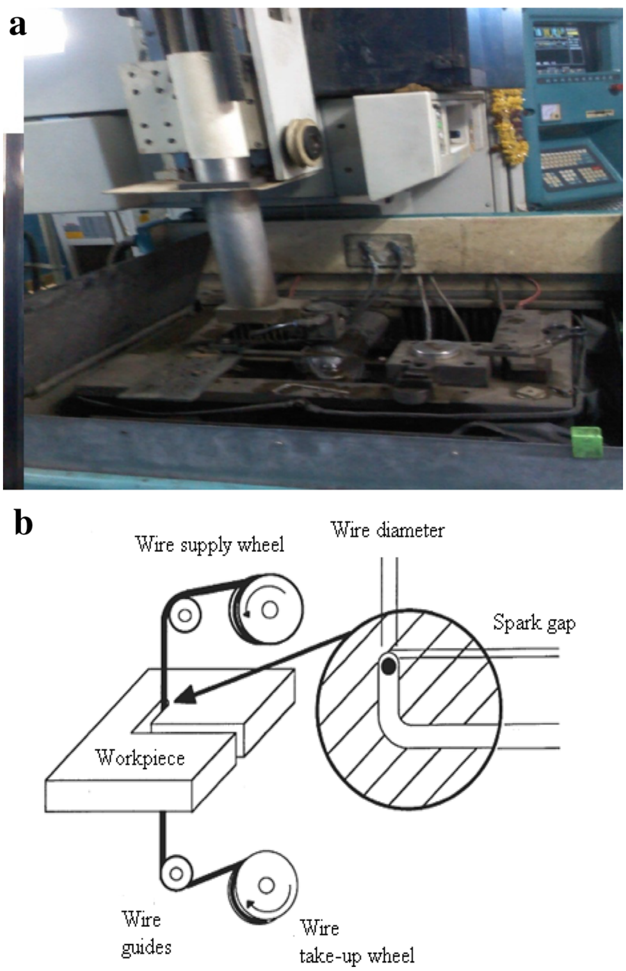


**Fig. 1** **a** Japax LDM 50 wire EDM machine, **b** Schematic diagram of wire EDM process

Taguchi L8 orthogonal array is considered for machining the specimens and the combinations of machining conditions are presented in Table 2.

### 2.3 Surface roughness

Surface roughness values are measured using stylus type profilometer, Mitutoyo SJ-310 with a cut off length of 0.8 mm measured along transverse direction of the machined surface.

### 2.4 Corrosion tests

The corrosion tests are conducted on the specimens machined by wire EDM at different conditions and also on the as received material. Pitting corrosion behavior is studied from the polarization curves obtained from electrochemical system of Gill AC unit used for conducting corrosion test. Figure 2 shows the basic electrochemical system with electrochemical flat cell used in this study. Saturated calomel is considered as reference electrode where as for auxiliary electrode, carbon is used. Corrosion testing is carried out in aerated 3.5% sodium chloride solution with an exposed area of the specimen as 1 $cm^2$. Potential scan of 0.166 mV per second is used with initial potential of – 0.25 V (OC) SCE to the final pitting potential.

## 3 Results and discussion

### 3.1 Corrosion

The corrosion resistance values of as received material and wire EDMed specimens at different machining conditions are presented in Table 3. Highest values of $E_{Corr}$ represent best corrosion resistance and vice versa. It can be observed that as the product of pulse on time and peak current

**Table 2** Machining conditions

| Machining conditions | Pulse on time ($T_{ON}$) µs | Peak current (IP) A | Servo voltage (SV) V | Wire tension (WT) Kg-f |
|---|---|---|---|---|
| 1 | 15 | 9 | 5 | 5 |
| 2 | 15 | 9 | 15 | 12 |
| 3 | 15 | 12 | 5 | 12 |
| 4 | 15 | 12 | 15 | 5 |
| 5 | 25 | 9 | 5 | 12 |
| 6 | 25 | 9 | 15 | 5 |
| 7 | 25 | 12 | 5 | 5 |
| 8 | 25 | 12 | 15 | 12 |

**Fig. 2** Electrochemical system of GILL AC unit

increases, corrosion resistance is observed to decrease. It can be clearly seen from the Table 3 that for the same values of the product of pulse on time and peak current, the $E_{Corr}$ values are also found to the same. Pulse on time and peak current are identified to be the most significant factors affecting the machining characteristics [34]. Servo voltage and wire tension has no significant effect on the machined surface properties.

## 3.2 Polarization curves

Figures 3a–d and 4, shows the polarization curves of the machined specimens and as received material respectively. The polarization curves for as received material and four cases of wire EDMed surfaces have been presented herein based on the discharge energy (product of pulse on time and peak current) at low values of cutting speed. However, the pitting corrosion potentials for all the cases are presented in Table 3. The machining condition at $T_{ON}=15$ µs, IP = 9A, SV = 15 V, WT = 12 kg-f with low level intensity of discharge energy with low cutting speed combination and is considered as Case-i. For intermediate values of different discharge energy levels, machining conditions $T_{ON}=15$ µs, IP = 12A, SV = 15 V, WT = 5 kg-f and $T_{ON}=25$ µs, IP = 9A, SV = 5 V, WT = 12 kg-f are considered as case-ii and case-iii respectively. The highest value of product of $T_{ON}$ and IP with low cutting speed is observed for the machining condition $T_{ON}=25$ µs, IP = 12A, SV = 5 V, WT = 5 kg-f and is considered as case-iv. The selected machining conditions cover all combinations of discharge energy intensity levels (all possible combinations of the product of pulse on time and peak current). Also from Table 3 it can be observed that for the same values of the product of pulse on time and peak current, the corrosion resistance values are almost same and hence the polarization curves of these four cases have been presented herein.

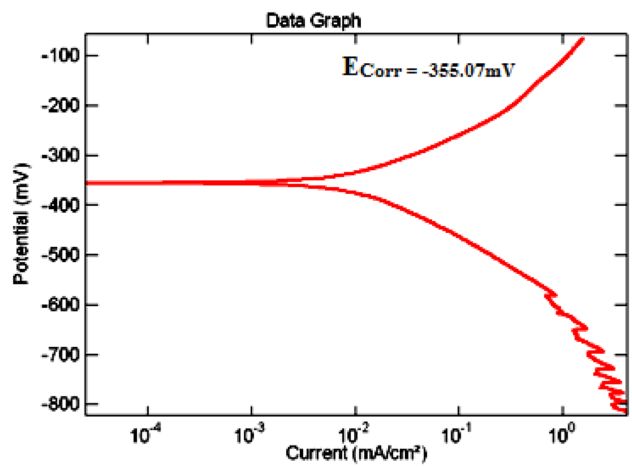


**Fig. 3** Potentiodynamic polarization curves of as received 316L SS material

**Table 3** Roughness and Corrosion values of 316 L SS material before and after wire EDM

| Machining condition | Pulse on time ($T_{ON}$) µs | Peak current (IP) A | Servo voltage (SV) V | Wire tension (WT) Kg-f | Cutting speed (Cs) mm/min | Surface roughness (µm) | E Corr (mV) |
|---|---|---|---|---|---|---|---|
| 1 | 15 | 9 | 5 | 5 | 1.41 | 2.69 | −251.24 |
| 2 | 15 | 9 | 15 | 12 | 1.23 | 2.22 | −246.07 |
| 3 | 15 | 12 | 5 | 12 | 1.36 | 2.25 | −355.08 |
| 4 | 15 | 12 | 15 | 5 | 1.29 | 2.35 | −359.14 |
| 5 | 25 | 9 | 5 | 12 | 1.52 | 2.96 | −365.34 |
| 6 | 25 | 9 | 15 | 5 | 1.78 | 2.85 | −367.26 |
| 7 | 25 | 12 | 5 | 5 | 2.2 | 3.42 | −370.08 |
| 8 | 25 | 12 | 15 | 12 | 2.32 | 3.32 | −369.18 |
| As received 316L SS material | | | | | | | −355.07 |

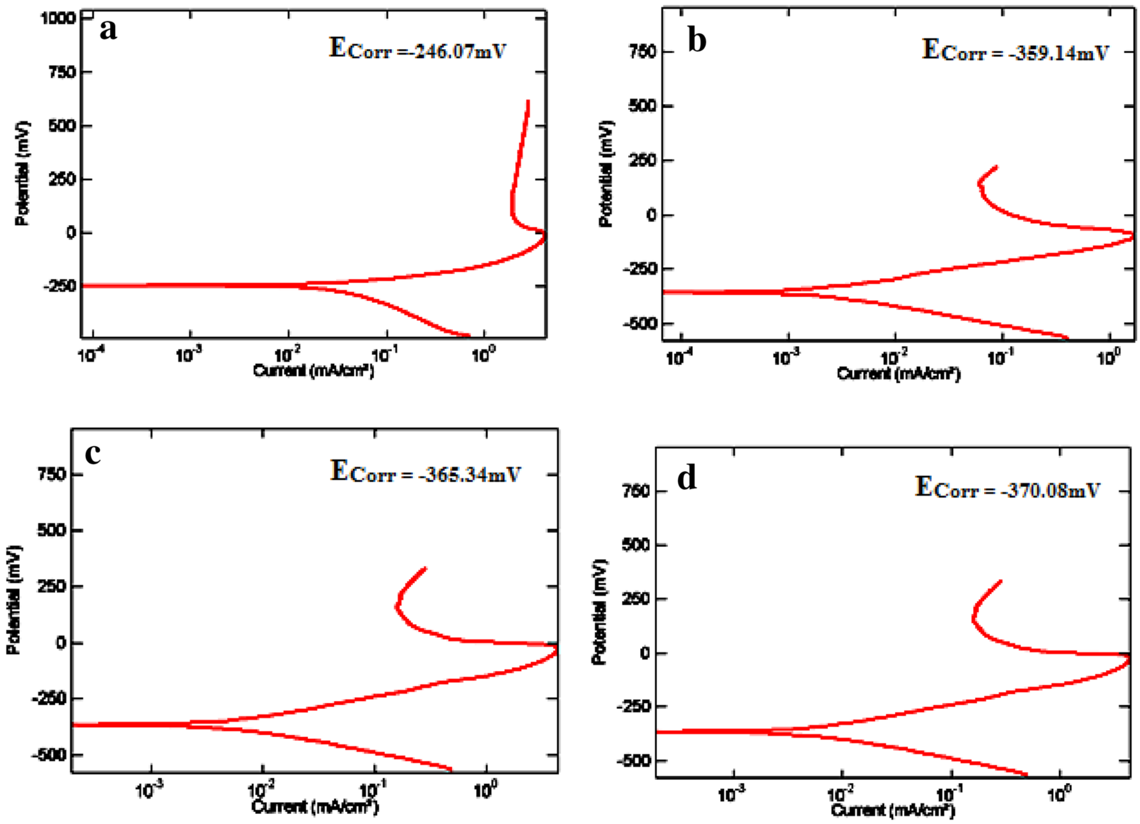


**Fig. 4** Potentiodynamic polarization curves of WEDMed specimen machined at **a** $T_{ON}=15$ µs, IP = 9A, SV = 15 V, WT = 12 kg-f **b** $T_{ON}=15$ µs, IP = 12A, SV = 15 V, WT = 5 kg-f **c** $T_{ON}=25$ µs, IP = 9A, SV = 5 V, WT = 12 kg-f **d** $T_{ON}=25$ µs, IP = 12A, SV = 5 V, WT = 5 kg-f

Figure 3a represents the polarization curve of wire EDMed specimen machined at $T_{ON}=15$ µs, IP = 9 A, SV = 15 V, WT = 12 kg-f. A pitting corrosion potential of – 246.07 mV is observed. A pitting corrosion potential of – 359.14 mV is observed when machined at $T_{ON}=15$ µs, IP = 12A, SV = 15 V, WT = 5 kg-f (Fig. 3b) and a pitting corrosion potential of -365.34 mV is observed at $T_{ON}=25$ µs, IP = 9A, SV = 5 V, WT = 12 kg-f (Fig. 3c) whilst a corrosion potential of -246.07 mV is observed at the machining condition $T_{ON}=25$ µs, IP = 12A, SV = 5 V, WT = 5 kg-f (Fig. 3d) and a corrosion potential of -355.07 mV has been noticed for as received 316L stainless steel material (Fig. 4) and rest of the values at other machining conditions are reported in Table 3. Higher the pitting corrosion potential value, the better is the corrosion resistance.

A high pitting corrosion potential of – 246.07 mV is observed at the machining condition in case-i and low corrosion potential of – 370.08 mV is observed in case-iv. From the above results it can be concluded that as the discharge energy increases the corrosion resistance decreases and this can be ascribed to the following reasons:

### 3.2.1 Corrosion behavior at low discharge energy

Due to high temperatures generated in wire EDM machining process the material melts and resolidifies results in the formation of white layer. When the specimens are machined at low discharge energy as in case-i, a thin white layer is observed on the machined surface. The cross sectional SEM image representing thin white layer is presented in Fig. 5. This thin passive white layer acts as a protective layer against corrosion attack in the medium. The white layer thus formed is composed of copper, copper oxide, iron carbide, chromium oxides and iron oxides which are evident from XRD patterns shown in Fig. 6. During the process of machining, the copper from brass wire electrode gets deposited on the machined surface forming protective layer. Similar phases were observed by [35, 36]. The presence of these phases was helpful in the increase in corrosion resistance of wire EDMed material. Works of Takakuwa et al. [37] demonstrated that, the residual stresses control the passivation layer formation and their retention. The surface layer possessing high residual stresses may lead to the formation of cracks thereby giving chance to decrease

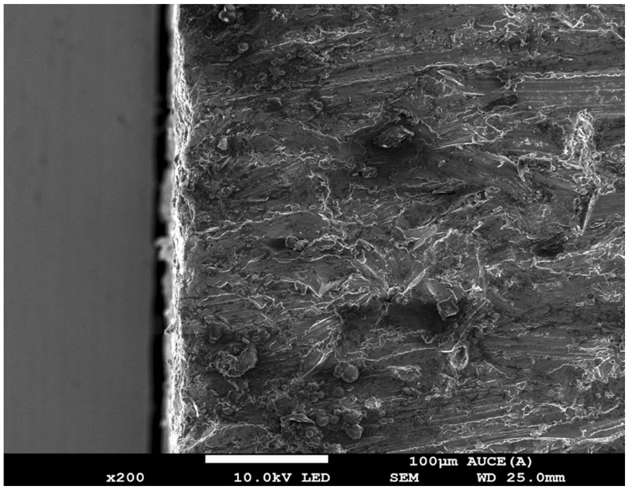


**Fig. 5** SEM image of WEDMed specimen at $T_{ON}=15$ µs, IP = 9A, SV = 15 V, WT = 12 kg-f

in corrosion resistance and hence low residual stresses are helpful to maintain good corrosion resistance. Also, from the works of Rao et al. [28] the wire EDM machining parameters with low level of discharge energy lead to the formation of thin white layer with low residual stresses on the machined surface. So this may also be the possible reason for increase in corrosion resistance of wire EDMed surface at low level of discharge energy due to the existence of thin passive layer. Figure 7 shows the SEM image after the corrosion test at this machining condition and it is observed that the surface is smooth and free from craters and debris with little evidence of pores and this smooth surface gave no provision for the corrosion solution to enter into the base metal and hence it offered good corrosion resistance.

#### 3.2.2 Corrosion behavior at high discharge energy

On the other hand, while machining with high discharge energy, a thick white layer is noticed on the surface which is shown in Fig. 8. With the increase in discharge energy, more amount of heat is transferred into the machining area and melting isothermals penetrate further into the interior of the material and the molten zone extends further into material resulting in a greater white layer thickness. On the white layer the deposition of copper from the wire electrode material is observed and the same phenomenon was identified by several authors [38–41]. The corrosion resistance at this machining condition is found to be low and this is due to fact that the depletion of more amount of chromium from the material and due to high amounts of deposition of oxides and carbides. These deposits on the surface are unable to act as a protective layer. Also, these depositions create more pores on the surface which can be observed from Fig. 9 and acts as a source for the corrosion media to attack the material. Due to high temperatures involved in high discharge energy the deposited copper gets oxidized and there by decreases the protective nature of the layer which eventually decreases corrosion resistance.

### 3.3 Surface morphology

Apart from the above mentioned discussion the corrosion resistance also depends on the surface morphology

**Fig. 6** XRD pattern of as received 316L SS material and WEDMed specimens

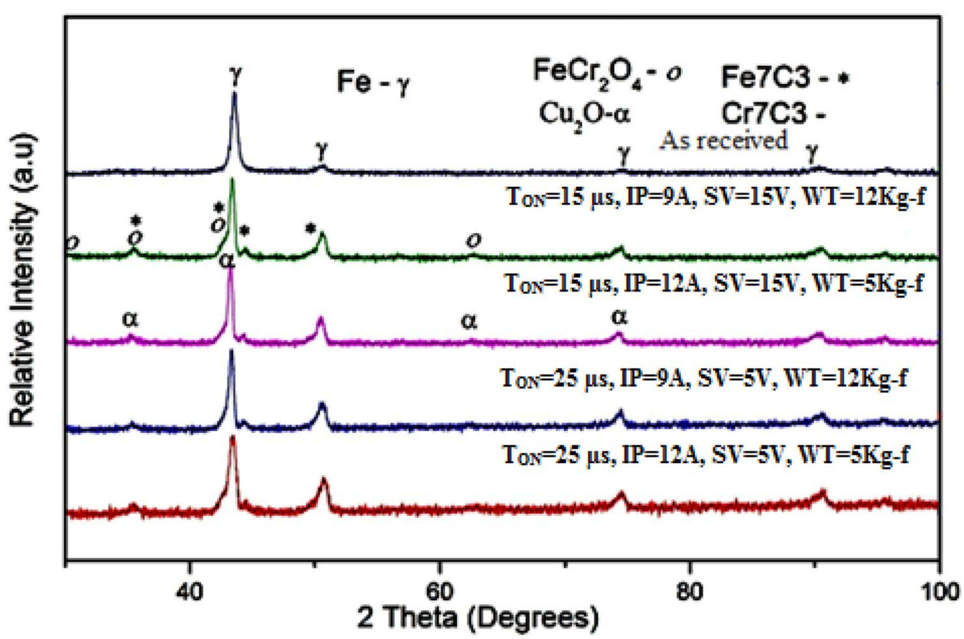

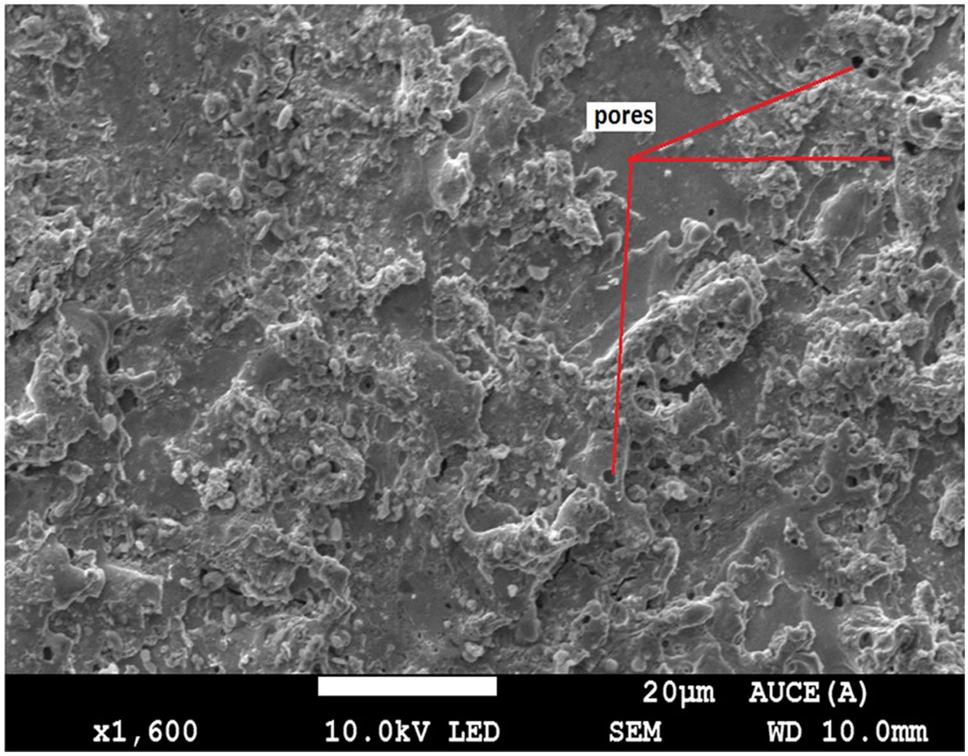


**Fig. 7** SEM image of WEDMed specimen at TON = 15 µs, IP = 9A, SV = 15 V, WT = 12 Kg-f after corrosion test

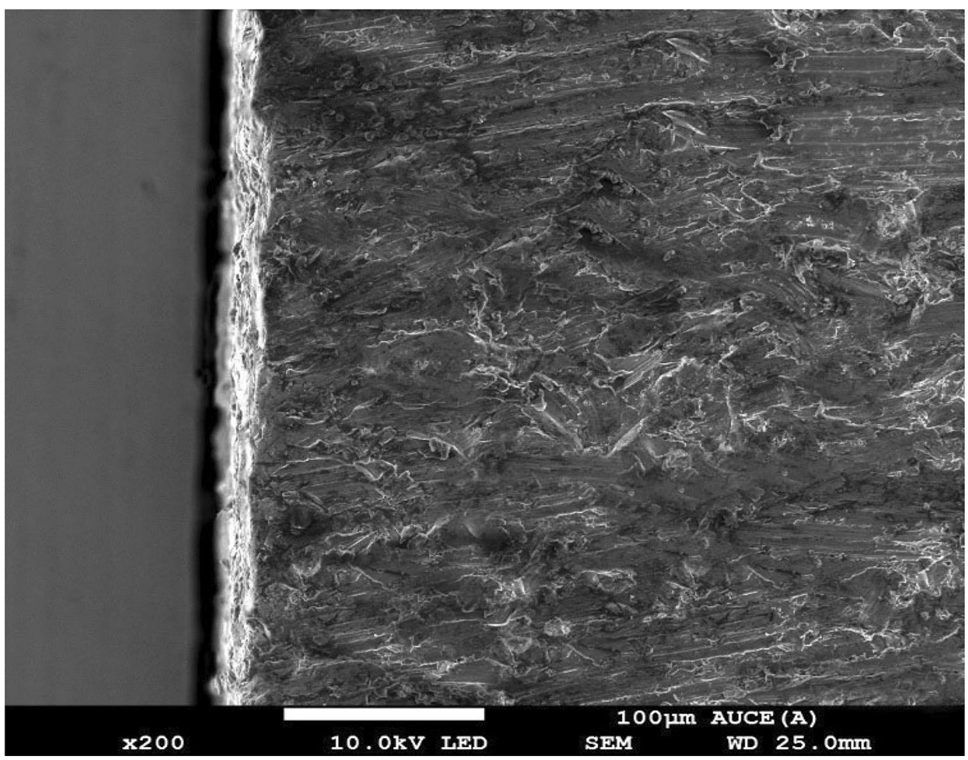


**Fig. 8** SEM image showing white layer at TON = 25 µs, IP = 12A, SV = 5 V, WT = 5 Kg-f

of the machined surface. At low levels of the product of $T_{ON}$ and IP, which is at the machining condition $T_{ON}$ = 15 µs, IP = 9A, SV = 15 V, WT = 12 kg-f, the roughness values is found to be low and the surface is found to be smooth with no evidence of debris, craters and cracks, this is due to fact that, the amount of thermal energy transferred to

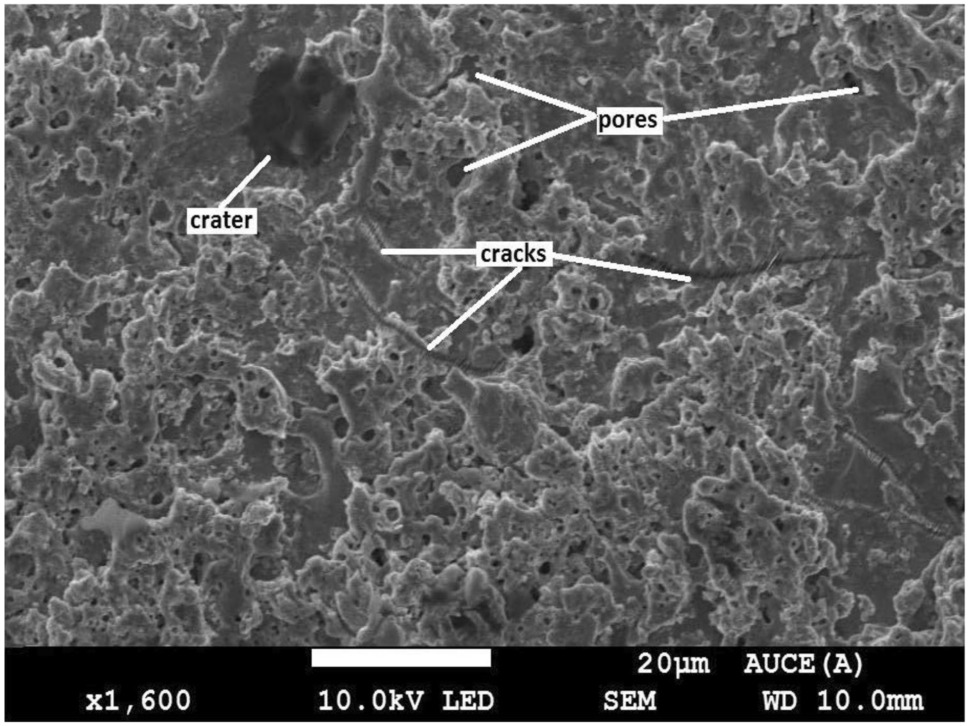


**Fig. 9** SEM image of WEDMed specimen at TON = 25 µs, IP = 12A, SV = 5 V, WT = 5 Kg-f after corrosion test

the machining area will be low and so less material will be melt. During solidification, a large amount of molten material is carried away from the surface by the dielectric present in the tank and the remaining material is solidified forming smooth surface [9]. The surface roughness value at this machining condition is observed to be 2.22 µ. This feature is evident from the SEM image shown in Fig. 10. Similar results have been reported by Gostimirovic et al. [42]. When machining at high discharge energy level i.e. $T_{ON}$ = 25 µs, IP = 12A, SV = 5 V, WT = 5 kg-f, the surface roughness is found to increase by 1.54 times, which may be due to the formation of craters, voids and the deposition of wire material. A large discharging energy causes violent sparks and impulsive forces and results in deeper and larger erosion crater on the surface. Also, during the cooling process of the molten material in the dielectric fluid, residues will remain at the periphery resulting in a rough surface. In addition to that, residual stresses are generated on the surface during the machining process and when these stresses exceed the ultimate tensile strength which eventually leads to the formation of cracks. The heating and cooling process of the surface result in a rapidly increase of yield stress. The areas that have been plastically transformed during the heating cannot flow back, so that plane tensile stresses build-up parallel to surface, resulting in cracks normal to the surface [43]. The crack distribution on the surface is observed and is evident from SEM micrograph shown in Fig. 11. At other machining conditions the roughness values was found moderate and are tabulated in Table 3. As explained earlier the surface roughness was also found to increase with the increase in discharge energy. Generally rough surfaces exhibit low pitting potential [44]. Hence it can be deduced that, the corrosion resistance decrease with increase in discharge energy.

## 4 Conclusions

The influence of WEDM parameters on the corrosion behavior of 316L stainless steel has been investigated in the present work. The parameters pulse on time and peak current are found to be significant factors affecting corrosion resistance of the machined surface. The surface roughness is found to increase with the increase in the product of pulse on time and peak current and vice versa. The thickness of white layer increases with the increase in the product of pulse on time and peak current. The white layer consists of carbides and oxides. The corrosion resistance found to increase with the decrease in the product of pulse on time and peak current. The increase in corrosion resistance is due to the formation of thin and stable protective layer on the surface at low values of pulse on time and peak current. The deposition of copper from wire electrode also enhanced the corrosion resistance of wire EDMed surface.

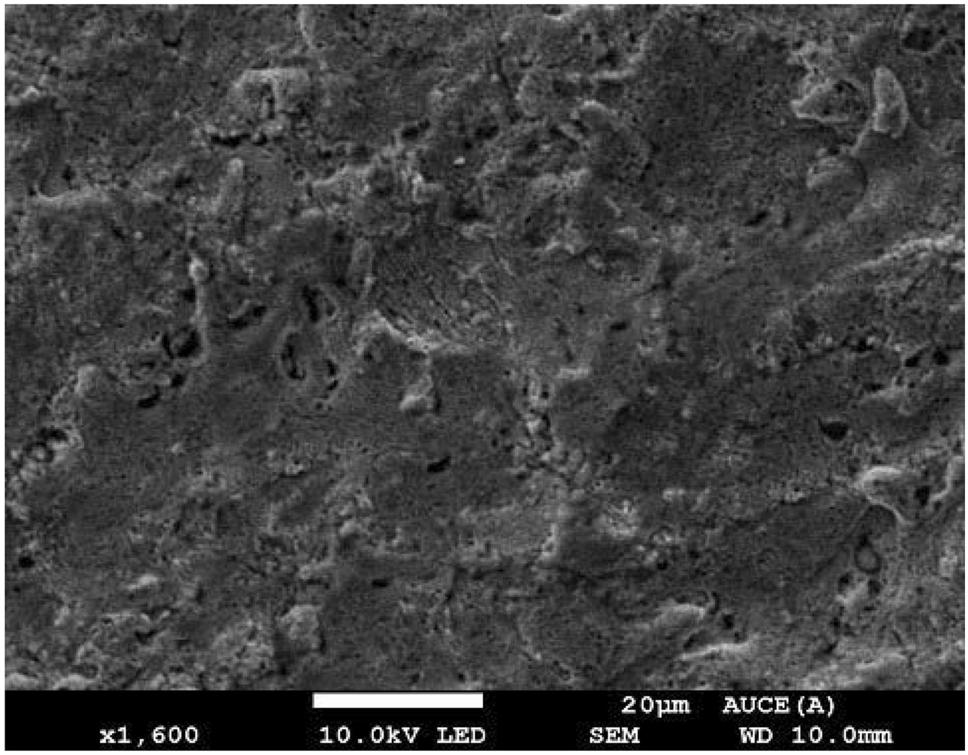


**Fig. 10** SEM image of WEDMed specimen at TON = 15 µs, IP = 9A, SV = 15 V, WT = 12 Kg-f

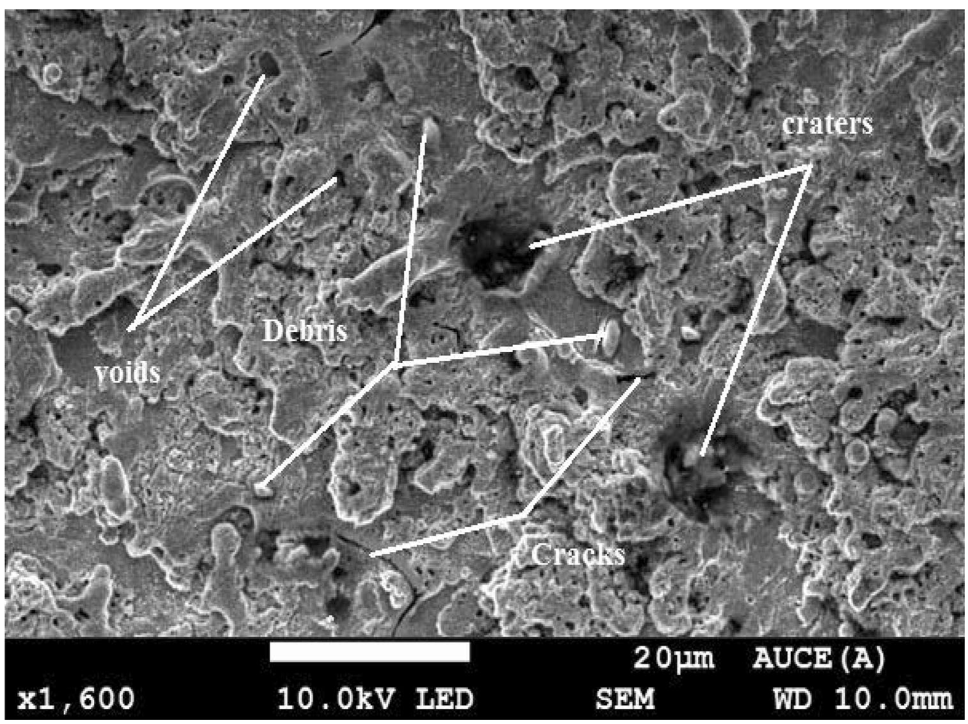


**Fig. 11** SEM image of WEDMed specimen at TON = 25 µs, IP = 12A, SV = 5 V, WT = 5 Kg-f

## Compliance with ethical standards

**Conflict of interest** The authors declare that they have no conflict of interest.

## References


1. Kanlayasiri K, Boonmung S (2007) Effects of wire EDM machining variables on surface roughness of newly developed DC 53 die steel: design of experiments and regression model. J Mater Process Technol 192(193):459–464
2. Azhiri RB, Teimouri R, Baboly MG, Leseman Z (2014) Application of Taguchi, ANFIS and grey relational analysis for studying, modeling and optimization of wire EDM process while using gaseous media. Int J Adv Manuf Technol 71:279–295
3. Sarkar S, Sekh M, Mitra S, Bhattacharyya B (2008) Modeling and optimization of wire electrical discharge machining of γ-TiAl in trimcutting operation. J Mater Process Technol 205:376–387
4. Lok YK, Lee TC (1977) Processing of advanced ceramics using the wire cut EDM process. J Mater Process Technol 63(1–3):839–843
5. Mohammadi A, Tehrani AF, Ehsan E, Davoud K (2008) A new approach to surface roughness and roundness improvement in wire electrical discharge turning based on statistical analyses. Int J Adv Manuf Technol 39:64–73
6. Sarkar S, Mitra S, Bhattacharyya B (2005) Parametric analysis and optimization of wire electrical discharge machining of γ-titanium aluminide alloy. J Mater Process Technol 159:286–294
7. Ahmet H, Caydas U (2004) Experimental study of wire electrical discharge machining of AISI D5 tool steel. J Mater Process Technol 148:362–367
8. Han F, Dingwen J, Jiang Y (2007) Influence of machining parameters on surface roughness in finish cut of WEDM. Int J Adv Manuf Technol 34:538–546
9. Li L (2013) Surface integrity characteristics in wire-EDM of Inconel 718 at different discharge energy. Procedia CIRP 6:220–225
10. Kiyak M, Cakir O (2007) Examination of machining parameters on surface roughness in EDM of tool steel. J Mater Process Technol 191(1–3):141–144
11. Yan BH, Tsai HC, Huang FY, Lee LC (2005) Examination of wire electrical discharge machining of $Al_2O_3$p/6061Al composites. Int J Mach Tools Manuf 45:251–259
12. Williams RE, Rajurkar KP (1991) Study of wire electrical discharge machined surface characteristics. J Mater Process Technol 281–2:127–138
13. Chen G, Wen X, Zhang N (1998) Corrosion resistance and ion dissolution of titanium with different surface micro roughness. Biomed Mater Eng 8:61–74
14. Newton TR, Shreyes NM, Thomas RW, Rosa MT, Laura R (2009) Investigation of the effect of process parameters on the formation and characteristics of recast layer in wire-EDM of Inconel 718. Mater Sci Eng AA513–AA514:208–215
15. Zinelis S (2007) Surface and elemental alterations of dental alloys induced by electro discharge machining (EDM). Dent Mater 23:601–607
16. Siva Prasad D, Shoba Ch, Rahul Varma K, Khurshid A (2015) Influence of wire EDM parameters on the damping behavior of A356.2 aluminum alloy. J Alloy Compd 646:257–263
17. Yan BH, Lin YC, Huang FY (2002) Surface modification of Al–Zn–Mg alloy by combined electrical discharge machining with ball burnish machining. Int J Mach Tools Manuf 42:925–934
18. Yu PH, Yang XL, Hsiang KL, Chao CM, Biing HY (2011) Improvement of wire electrical discharge machining efficiency in machining polycrystalline silicon with auxiliary-pulse voltage supply. Int J Adv Manuf Technol 57:991–1001
19. Ghanem F, Braham C, Sidhom H (2003) Influence of steel type on electrical discharge machined surface integrity. J Mater Process Technol 142:163–173
20. Kuriakose Shajan, Shunmugam MS (2004) Characteristics of wire-electro discharge machined Ti6Al4 V surface. Mater Lett 58:2231–2237
21. Ekmekci B, Gungor E (2015) Wear resistance of electrical discharge machined surfaces. In: Akademik Platform, ISITES Valencia-Spain, pp. 1080–1089
22. Kuriachen B, Lijesh KP, Kuppan P (2018) Multi response optimization and experimental investigations into the impact of wire EDM on the tribological properties of Ti–6Al–4 V. Trans Indian Inst Met 71(6):1331–1341
23. Prasad DS, Ebenezer NS, Shoba Ch, Raju P, Rao PS (2018) The effect of T6 heat treatment on corrosion behavior of nickel electroplated metal matrix composites. Silicon (in press)
24. Badran Omar, Kloub Naser, Al-Tal Musa (2008) The effect of shot peening and polishing on the pitting corrosion resistance of stainless steel. Am J Appl Sci 5(10):1397–1402
25. Razavi Shoja, Gordani Gholam Reza, Ma HC (2011) A review of the corrosion of laser nitride Ti6Al4 V. Anti Corros Methods Mater 58(3):140–154
26. Akasakal B, Gavgalii M, Dikici B (2010) The effect of coating thickness on corrosion resistance of hydroxyapatite coated Ti6Al4 V and 316L SS implants. J Mater Eng Perform 19(6):894–899
27. Tiwari SK, Mishra T, Gunjan MK, Bhattacharyya AS, Singh TB, Singh R (2007) Development and characterization of sol–gel silica alumina composite coating on AISI 316L for implant applications. Surf Coat Technol 201:7582–7588
28. Feng K, Xun C, Zhuguo L, Paul KC (2012) Improved corrosion resistance of stainless steel 316L by Ti ion implantation. Mater Lett 68:450–452
29. Prasad DS, Ebenezer NS, Shoba Ch (2017) The effect of nickel electroplating on corrosion behavior of metal matrix composites. Trans Indian Inst Met 70(10):2601–2607
30. Yue TM, Yan LJ, Man HC (2004) The effect of machined surface condition on the corrosion behavior of magnesium ZM51/SiC composite. Mater Manuf Process 19(2):123–138
31. Rao PS, Ramji K, Satyanarayana B (2016) Effect of wire EDM conditions on generation of residual stresses in machining of aluminum 2014 T6 alloy. Alex Eng J 55(2):1077–1084
32. Mahapatra SS, Patnaik A (2007) Optimization of wire electrical discharge machining (WEDM) process parameters using Taguchi method. Int J Adv Manuf Technol 34(9–10):911–925
33. Raju P, Sarcar MMM, Satyanarayana B (2014) Optimization of wire electric discharge machining parameters for surface roughness on 316L stainless steel using full factorial experimental design. Procedia Mater Sci 5:1670–1676
34. Raju P, Ratnam Ch, Prasad DS (2018) Surfce integrity analysis and simultaneous optimization using Taguchi grey relational analysis. Int J Adv Sci Technol 114:11–22
35. Sidhom H, Farhat G, Tidiane A, Gonzalo G, Chedly B (2013) Effect of electro discharge machining (EDM) on the AISI316L SS white layer microstructure and corrosion resistance. Int J Adv Manuf Technol 65:141–153
36. Cusanelli G (2004) Microstructure at submicron scale of the white layer produced by EDM technique. J Mater Process Technol 149:289–295
37. Takakuwa O, Hitoshi S (2015) Effect of residual stress on the corrosion behaviour of austentitic stainless steel. Adv Chem Eng Sci 5:62–71

38. Boujelbene M, Bayraktar E, Tebni W, Ben Salem S (2009) Influence of machining parameters on the surface integrity in electrical discharge machining. Arch Mater Sci Eng 37(2):110–116
39. Hascalık A, Caydas U (2007) Electrical discharge machining of titanium alloy (Ti–6Al–4V). Appl Surf Sci 253:9007–9016
40. Lee HT, Hsu FC, Tai TY (2004) Study of surface integrity using the small area EDM process with a copper–tungsten electrode. Mater Sci Eng 364:346–356
41. Ramasawmy H, Blunt L, Rajurkar KP (2005) Investigation of the relationship between the white layer thickness and 3D surface texture parameters in die sinking EDM process. Precis Eng 29:479–490
42. Gostimirovic M, Pavel K, Milenko S, Branko S (2012) Influence of discharge energy on machining characteristics in EDM. J Mech Sci Technol 26(1):173–179
43. Theisen W, Schuermann A (2004) Electro discharge machining of nickel–titanium shape memory alloys. Mater Sci Eng 348(A):200–204
44. Laycock NJ, Newman RC (1997) Localised dissolution kinetics, salt films and pitting potentials. Corros Sci 39:1771–1790